photonics

MDPI

Article

Superluminescent Diodes Based on Chirped InGaAs/GaAs Quantum Well-Dot Layers

Mikhail V. Maximov [1,*], Nikita Yu. Gordeev [2], Yuri M. Shernyakov [2], Grigoriy O. Kornyshov [1], Artem A. Beckman [2], Alexey S. Payusov [2], Sergey A. Mintairov [2], Nikolay A. Kalyuzhnyy [2], Marina M. Kulagina [2] and Alexey E. Zhukov [3]

[1] Nanophotonics Laboratory, Alferov University, St. Petersburg 194021, Russia; supergrigoir@gmail.com
[2] Ioffe Institute, St. Petersburg 194021, Russia; gordeev@switch.ioffe.ru (N.Y.G.); yuri.shernyakov@mail.ioffe.ru (Y.M.S.); spbgate21@gmail.com (A.A.B.); plusov@mail.ioffe.ru (A.S.P.); mintairov@scell.ioffe.ru (S.A.M.); marina.kulagina@mail.ioffe.ru (M.M.K.)
[3] School of Physics, Mathematics, and Computer Science, HSE University, St. Petersburg 190008, Russia; aezhukov@hse.ru
* Correspondence: maximov.mikh@gmail.com

Abstract: We study the applicability of InGaAs/GaAs quantum well-dots (QWDs) for active regions of broadband superluminescent diodes (SLDs) emitting in the 950–1150 nm spectral range; 2 mm long SLDs with a bent section and an active region based on seven chirped QWD layers show emission spectra centered at 1030 nm with a full-width at half-maximum of 80 nm and an output power of 2 mW. In a 250 μm long SLD with a tilted stripe that has an increased output loss, the width of the emission spectra is 113 nm at 20 °C and 120 nm at 60 °C.

Keywords: superluminescent diode; quantum well-dots; broadband emission

Citation: Maximov, M.V.; Gordeev, N.Y.; Shernyakov, Y.M.; Kornyshov, G.O.; Beckman, A.A.; Payusov, A.S.; Mintairov, S.A.; Kalyuzhnyy, N.A.; Kulagina, M.M.; Zhukov, A.E. Superluminescent Diodes Based on Chirped InGaAs/GaAs Quantum Well-Dot Layers. *Photonics* **2023**, *10*, 1090. https://doi.org/10.3390/photonics10101090

Received: 24 August 2023
Revised: 16 September 2023
Accepted: 25 September 2023
Published: 28 September 2023

1. Introduction

Superluminescent diodes (SLDs) are of considerable interest for investigating the fundamental principles of light emission and amplification in material, as well as for their numerous applications in the present and future advanced optical systems. SLDs emitting in the optical range of 950–1150 nm are of great importance for optical coherence tomography (OCT) systems, which can scan the retina and other organs mainly consisting of water [1,2]. Another important application of SLDs of this optical range is fiber gyroscopes for unmanned ground transport systems. The near-infrared spectral range is relatively eye-safe, and the use of cheap silicon photodetectors and CCD arrays makes such systems cost-efficient and convenient for mass production. SLDs are also promising for optical data transmission, random number generation and spectroscopy. From the viewpoint of most applications, the general requirements for SLDs are the following: (i) the emission spectrum has a large width, (ii) there are no significant intensity modulations (maxima and dips), and (iii) high output power. The requirements regarding a broad emission spectrum and high output power are somehow contradictory. With the growth in the injection current, light amplification arises, and a positive optical feedback caused by partial light reflection from device facets results in an increase in emission intensity in a narrow spectral range close to the gain maximum. This process eventually results in lasing. To suppress the optical feedback, prevent lasing, provide broadband superluminescent emission and increase output power, several SLD designs have been developed and studied: antireflection coatings, ridge waveguides tilted by 5–10 degrees with respect to cleaved facets [3,4], tilted and tapered ridge waveguides [5–7], bent ridge waveguides [8,9], and multi-section designs [10–12] including integrated optical amplifiers [6,13].

Traditionally, InGaAs/GaAs quantum wells (QWs) are used as active regions of SLDs emitting in the spectral range from 950 to 1100 nm. However, the width of QW emission

spectra is not large—typically from 10 to 15 nm. The growth of multiple QWs requires the use of sophisticated strain-reduction epitaxial techniques. In QW SLDs, a strong decrease in carrier density in the direction from p-cladding to n-cladding has been observed [14]. As a result, QWs situated closer to p-cladding make the strongest contribution to the emission spectra. In [15], GaAs-based bipolar cascade SLDs with the active region based on four InGaAs/GaAs quantum wells (QWs) were investigated. The tunnel junction was aimed to minimize the nonuniform carrier distribution between multiple QWs. The QW ground state (GS) transition emission wavelengths were 1050, 1100, 1000 and 950 nm (listed according to the positions from the n-cladding to the p-cladding). The full-width at half-maximums (FWHM) of the optical emission spectra obtained for the 1 mm long device under a large range of CW bias driving currents were from 170 to 180 nm, and the maximal output power was 0.65 mW. A higher output power of 19 mW was obtained in a pulse mode, but the FWHM was much smaller (14 nm).

InGaAs/GaAs self-organized quantum dots (QDs) have been shown to be very advantageous as the active region of broadband SLDs. Inhomogeneous broadening of the QD array results in a large width of QD emission spectra, which is typically about 60 nm. Very broad and smooth emission spectra without significant intensity modulations can be implemented by using so-called chirped active regions. In this case, peaks of the GS emission of individual QD layers are shifted to fill the gaps between the ground and excited states of the other QD layers [4,16,17]. InAs/InGaAs/GaAs QDs obtained by overgrowth of initial Stranski–Krastanov islands with a thin InGaAs layer [18] and referred to as dot-in-well (DWELL) have been widely used as the active region of near-infrared SLDs. The largest bandwidths have been demonstrated for SLDs with central emission wavelengths in the optical range of about 1.2 μm [12,19]. In [19], 5 μm wide and 2 mm long SLDs with the active region based on one $In_{0.34}Ga_{0.66}As$ QW and six chirped InAs/InGaAs/GaAs DWELL layers were studied. The stripes were tilted at 7° to inhibit lasing. The devices demonstrated a 3 dB linewidth of 290 nm centered at 1.2 μm, with 2.4 mW output power at room temperature.

Present SLDs with a central wavelength of 1.0–1.1 μm have narrower optical bandwidth than their longer-wavelength (~1.2 μm) counterparts. In [16], high-power SLDs utilizing a three-stacked InGaAs/GaAs QD formed by a short-period superlattice of InAs and GaAs have been demonstrated. The QD SLD was fabricated in the form of a 7-degree tilted triangular p-electrode. The output power and the spectral bandwidth of the QD SLD were 0.9 W and 80 nm, respectively. In [5], SLDs utilizing multiple layers of dots of tuned height have been reported. The active region of the devices consisted of two repetitions of four layers of InAs quantum dots with 30 nm thick GaAs barrier/cap layers within a 300 nm waveguide. The SLDs were made in a tilted and tapered waveguide design [12] with a 1 mm long waveguide and with tilted and tapered angles of 8° and 2°, respectively. The resulting width of the output facet was 35.49 μm. The device exhibited a 3 dB bandwidth of 190 nm with a central wavelength of 1020 nm under continuous wave (cw) conditions. The maximum corresponding output power achieved in these devices under cw and pulsed operation conditions were 0.54 mW and 17 mW, respectively. Rapid thermal annealing can be used to shift the emission spectra of InGaAs/GaAs QD to shorter wavelengths closer to 1 μm. In [7], broadband SLDs with the active region based on multiple QD layers subjected to rapid thermal annealing were reported. A design with a tilted tapered lateral waveguide, non-pumped absorbing region, and V-groove was used. The devices exhibited a 3 dB emission bandwidth of 146 nm centered at 984 nm with a CW output power of 15 mW at room temperature.

Recently, a novel type of active region referred to as InGaAs/GaAs quantum well-dots (QWDs) was developed [20]. QWDs represent an array of indium-rich 3D islands located inside the indium-depleted residual InGaAs/GaAs layer. The QWDs can be considered as nanostructures of mixed (0D/2D) dimensionality. On the one hand, they represent a dense QD array with relatively low confinement energies for electrons and holes. On the other hand, they can be viewed as strongly modulated in composition and thickness QW. QWDs

have some advantages intrinsic to both QDs and QWs. For example, QWDs have a record high optical gain and broader emission spectra as compared with QWs [21]. The possible dislocation-free growth of at least 15 QWD layers in the active region, which can be chirped in indium content and/or effective thickness, enables high-intensity stimulated emission with broad spectra without pronounced intensity modulations. Another advantage of the QWDs is reduced charged carrier transport in the lateral direction [20]. This effect decreases non-radiative recombination at light-emitting device cleaved facets and, thus, potentially facilitates achieving higher output power and longer lifetime. Suppression of carrier lateral transport also makes it possible to deeply etch QWD-based devices through the active region, which can be useful for the fabrication of narrow stripe single mode SLDs in deep mesa geometry. In [22], we reported on 2 mm long SLDs with one QWD layer in the active region that exhibited a stimulated emission spectrum centered at 1050 nm with a maximal 3 dB bandwidth of 36 nm and pulsed output power of 17 mW. In this paper, we report on fabrication and studies of SLDs based on chirped QWD layers and demonstrate that this approach is promising for increasing the emission bandwidth.

2. Materials and Methods

The SLDs were fabricated from a laser wafer with seven chirped QWD layers (7QWD) in the active region. The wafer was grown by MOCVD on a (100) GaAs substrate misoriented by 6° towards (111). The QWD layers were formed by the deposition of $In_{0.4}Ga_{0.6}As$ with the changing thickness in order to cover a spectral range from 920 to 1070 nm. The active region of the SLDs under study is based on seven chirped QWD layers (Figure 1a). The nominal thicknesses of the individual QWD layers in the active region listed in the direction from the *n*-cladding to the *p*-cladding and corresponding emission wavelengths (Figure 1b) were the following: 2 monolayers (MLs) (920 nm), 3 MLs (945 nm), 4 MLs (980 nm), 5 MLs (1010 nm), 6 MLs (1035 nm), 7 MLs (1055 nm) and 9 MLs (1070 nm). Individual QWD layers were separated with 40 nm thick GaAs spacers. The active region was placed in the center of 0.44 μm thick GaAs waveguide. The waveguide was sandwiched between *p*- and *n*-type $Al_{0.25}Ga_{0.75}As$ cladding layers having thicknesses of about 1.2 μm. A 50 nm thick InGaP etch-stop layer was inserted into the *p*-cladding at a distance of 260 nm from the waveguide. A 200 nm thick *p*+-GaAs cap layer was grown on the top of *n*-type $Al_{0.25}Ga_{0.75}As$ cladding. In the following, we will refer to the individual QWD layer formed by the deposition of *N* monolayers of $In_{0.4}Ga_{0.6}As$ as "*N*ML-QWDs" for short. A reference epitaxial wafer with a single QWD layer formed by the deposition of 8 MLs of $In_{0.4}Ga_{0.6}As$ was also grown. It has a 550 nm wide GaAs waveguide and the same claddings as the chirped SLDs. The structure was aimed to investigate the emission spectra of individual QWD layers.

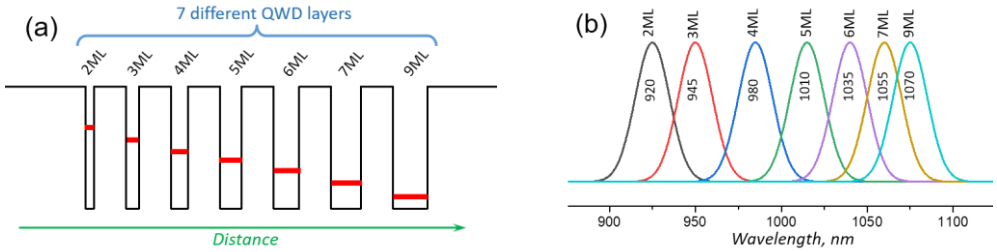

Figure 1. Schematic images of the SLD active region (**a**) and corresponding emission spectra (**b**).

Two types of SLDs were processed by using standard optical lithography and reactive ion etching. In both cases, SLD width was 5 μm. The etching depth of 950 nm was set by the etch-stop layer. AgMn/Ni/Au contacts were formed on top of the *p*+-GaAs cap layers. Then, the GaAs substrate was thinned down to 100 μm, and an AuGe/Ni/Au contact was deposited onto the *n*-side of the GaAs substrate. The first SLD design represents 2 mm long stripe with 350 μm long bent section having derivation angle of 7° and is referred to as a J-stripe. The bent section is aimed to suppress the optical feedback and prevent lasing [8,9]. The other design represents 250 μm long stripes tilted by 7° to the as-cleaved

facets. These SLDs with short cavities have high output loss, so the lasing is eliminated up to the high pumping currents. No antireflection facet coatings were used in all samples. The processed SLDs were cleaved into individual chips and mounted on copper heatsinks by indium solder. The devices were studied in a pulsed mode (300 ns, 3 kHz) to prevent device overheating.

3. Results and Discussion

Reference SLDs based on one QWD layer show very broad spectra with maximal full-width at half-maximum (FWHM) of 125 nm (Figure 2). In the range of injection currents from 100 to 300 mA, the FWHM is above 120 nm. In contrast to the case of QDs and QWs, the spectra show no pronounced peaks associated with the ground and excited states. This means that in designing chirped QWD active regions, it is not necessary to precisely fill in the spectral dips between the ground and excited states of an individual QWD layer by emission peaks of another QWD layer as it is necessary in the case of QDs. There is no saturation of the GS peak, and the spectra remain "flat-topped" (no pronounced spectral maxima and dips), at least in the pumping current range of 30–150 mA. The output power of this short SLD with one QWD layer was 0.68 mW per facet at 300 mA. A drawback of SLDs based on one QWD layer (or several identical QWD layers) is that high pumping currents are required to fill in with carriers high-energy states responsible for the short wavelength part of the emission spectra. Thus, the performance of such SLDs is doubtful for their practical applications. So, usually, multilayer active regions consist of layers emitting at different wavelengths, as the one investigated in this work. Figure 3a shows the evolution of the electroluminescence spectra of the 2 mm long J-stripe of the SLD with the active region based on seven chirped QWD layers with an increase in the pumping current. Nominal spectral positions of the photoluminescence maxima of individual QWD layers are shown by vertical lines. These positions were determined by photoluminescence studies of the test samples with a single QWD layer formed by different amounts of deposited $In_{0.4}Ga_{0.6}As$. However, we note that in the multilayer SLDs, the positions of emission spectra maxima of individual QWD layers may slightly change due to strained fields induced by neighboring QWD layers as compared to the case of samples with a single QWD layer. The total SLD spectrum is a superposition of the emission lines of seven individual QWD layers in the active region. However, their relative contribution depends on the injection current and temperature. At low pumping currents, only QWD layers emitting at longer wavelengths contribute to the spectra, and the FWHM of the emission line is about 50 nm (Figure 3b). With an increase in pumping currents, the population of QWD layers emitting at shorter wavelengths increases, and the spectra broaden. At high pumping currents, the peak of the whole emission spectrum is at ~1000 nm. This peak is formed by the ground state emission of 4ML-QWDs (980 nm), 5ML-QWDs (1010 nm) and 6ML-QWDs (1035 nm) and the excited states of 7ML-QWDs (1055 nm) and 9ML-QWDs (1070 nm). Thus, this emission peak is supposed to correspond to the spectral position of the highest integral density of states of the active region. The full-width at half-maximum (FWHM) of the SLD spectra grows from 48 to 80 nm with an increase in the pumping current and then decreases down to 56 nm (Figure 3b). At currents above 500 mA, a transition from spontaneous emission to lasing accompanied by the narrowing of the emission line takes place (not shown in the figure). The pumping current dependence of the output power shows a superlinear behavior typical for SLDs (Figure 3). The SLD output optical power per facet is 1.2 mW at the pumping current of 300 mA and 2.2 mW at 500 mA.

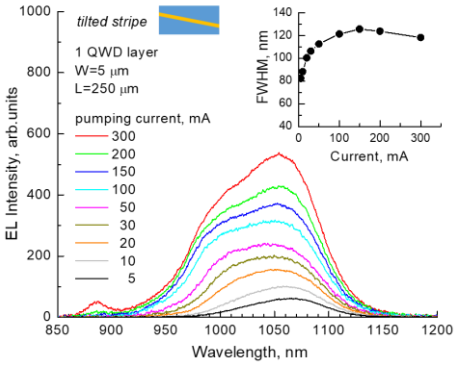

Figure 2. Electroluminescence spectra and their FWHMs (inset) of a 250 μm long reference SLD with active region based on one QWD layer at various pumping currents.

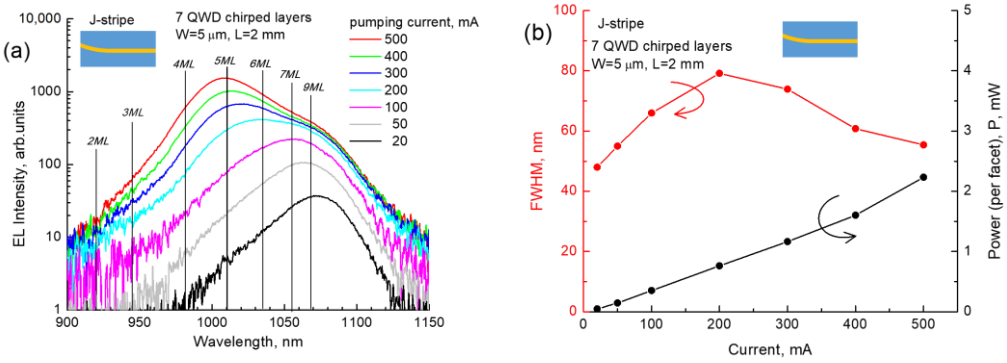

Figure 3. (**a**) Electroluminescence spectra of the SLD with the active region based on seven chirped QWD layers in J-stripe geometry (cavity length 2 mm) at various pumping currents. The vertical lines mark nominal positions of the photoluminescence maxima of the individual QWD layers in the active region. (**b**) Pumping current dependences of the FWHM of the emission spectrum and the optical power per facet.

The performance of the SLDs under study is limited mainly by their simple cavity design. According to our near-field studies, the bent ridge waveguide requires optimization for better light guiding. In up-to-date SLDs, antireflection coatings are usually used to suppress lasing at high pumping currents and prevent the narrowing of the emission spectra. Modern SLDs have large lengths (4–6 mm) and tapered and/or multi-section designs to increase output power [6,13]. We expect that using the mentioned in the introduction up-to-date cavity designs [5–7,10–13] would allow for increasing output power of the QWD-based SLDs.

To assess the potential of the chirped QWD active region for providing broadband emission, we studied SLDs with the active region based on seven chirped QWD layers having cavity lengths as short as 250 μm fabricated in a tilted geometry. In this case, the output loss is very high, and the stimulated emission regime is maintained up to high pumping currents. At the pumping current of 300 mA, the ground states of five individual QWD layers in the active region, namely 4ML-QWDs (980 nm), 5ML-QWDs (1010 nm), 6ML-QWDs (1035 nm), 7ML-QWDs (1055 nm) and 9ML-QWDs (1070 nm)), mainly contribute to the emission spectrum, which results in its FWHM as large as 113 nm (Figure 4a). The QWD layers emitting at short wavelengths (2ML-QWDs (920 nm) and 3ML-QWDs (945 nm)) marginally contribute to the total stimulated emission spectrum. This effect can be explained by two reasons. Firstly, in a multilayer active region, carrier density decreases with an increase in the distance from the *p*-cladding [14]. As a result, the QWD layers closest to the *p*-cladding make the major contribution to the SLD spectra. Secondly, charge carriers are accumulated in the QWD layers with the highest confinement

energy emitting at the longest wavelengths, so the emission of the shorter-wavelength QWD layers is weaker. The output power of this short SLD is rather low—0.5 mW per facet.

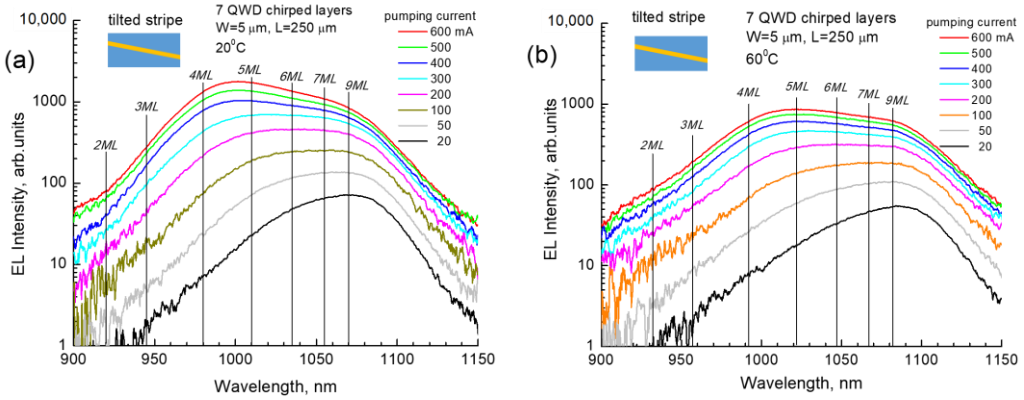

Figure 4. Electroluminescence spectra of the SLD with the active region based on seven chirped QWD layers in tilted stripe geometry (cavity length 250 μm) at various pump currents at 20 °C (**a**) and 60 °C (**b**). In panel (**a**), the vertical lines mark the positions of the nominal maxima of the photoluminescence spectra of the individual QWD layers measured at 20 °C. For the spectra measured at 60 °C in panel (**b**), the vertical lines are redshifted by 12 nm, which corresponds to the GaAs bandgap shift induced by the temperature growth from 20 °C to 60 °C.

In [23], SLD operation at strongly increased temperatures was proposed to realize large spectral bandwidth. The temperature-dependent performance of InAs/GaAs QD-based SLDs with 2000 μm long, 5 μm wide ridge waveguides tilted by 7° and composed of eight multi-sections were investigated. At 180 °C, the devices exhibited a 3 dB linewidth of 270 nm and a power of 0.34 mW. However, the degradation characteristics of the SLD operating at such high temperatures were not reported. We studied the performance of the SLDs with active regions based on seven chirped QWD layers at 60 °C, which corresponds to a typical overheating of operating electronic boards. Figure 4 shows the evolution of the electroluminescence (EL) spectra at 20 °C and 60 °C with an increase in the pumping current. At 20 °C, the FWHM grows up to 112 nm when increasing the pumping current up to 300 mA and then slightly decreases down to 100 nm with further increasing the pumping current from 300 mA up to 600 mA. At 60 °C, the maximal FWHM of 120 nm is achieved at 200 mA and remains unchanged (Figure 5a). At 20 °C, the output power grows superlinearly with an increase in the pumping current. The maximal achieved output power slightly exceeds 1 mW. In contrast, the light-current characteristic at 60 °C shows sublinear growth that can be attributed to a higher current of stimulated emission onset. Maximal output power at 60 °C is lower than at 20 °C (0.6 mW vs. 1.1 mW at 600 mA, respectively). The normalized EL spectra at 20 °C and 60 °C at the pumping current of 300 mA are compared in Figure 5b. For better comparison of the line shapes of emission spectra at 20 °C and 60 °C, the spectrum at 60 °C is shifted to shorter wavelengths to the value corresponding to the temperature shift of GaAs bandgap (0.3 nm/K·40 K = 12 nm). The increased temperature results in a broadening of the long-wavelength shoulder of the EL spectra. This effect can be attributed to the temperature escape of charge carriers from the QWD layers with lower confinement energy of electrons and holes and following recapture by the ones with high confinement energy, which results in a stronger contribution of 9ML-QWDs (1070 nm).

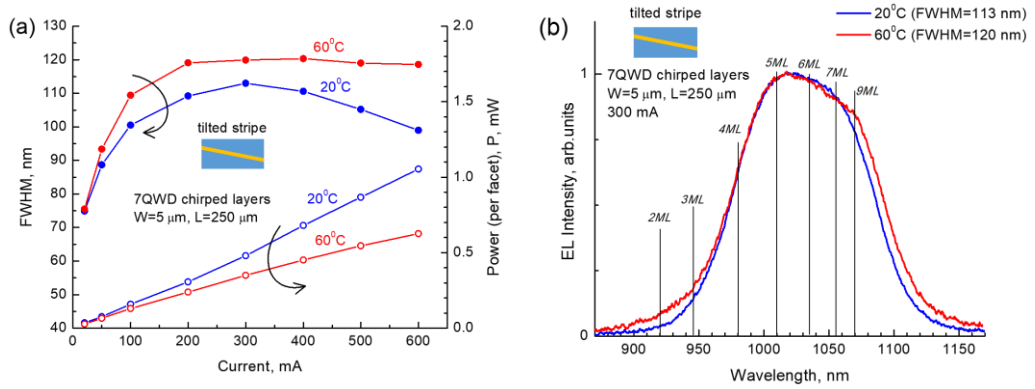

Figure 5. (**a**) Pumping current dependencies of the FWHM (solid circles) and optical power per facet (open circles) at 20 °C and 60 °C of the SLD with the active region based on seven chirped QWD layers in tilted stripe geometry (cavity length 250 μm). (**b**) The normalized EL spectra at 20 °C and 60 °C at the pumping current of 300 mA of the same SLD. The spectrum at 60 °C is blueshifted by 12 nm.

4. Conclusions

To conclude, we demonstrated that the quantum well-dots are very promising as active regions for SLDs emitting in the spectral range of 950–1150 nm with large bandwidth. Stimulated emission spectra in the devices with high output loss are 113 nm wide at 20 °C. Despite the fact that the performance of our present SLDs with simple cavity design lags behind that of the best counterparts, we believe that QWDs potentially offer some advantages over InGaAs/GaAs self-organized QDs for high-power broadband SLDs. Due to limited QD density and inhomogeneous broadening of the QD array, its density of state is lower than that in QWs and QWDs. Moreover, in QDs emitting near 1.1 μm, the localization energy of electrons and holes at the ground state is relatively low and thermal carrier escape to higher energy levels is pronounced. Both facts can result in a saturation of the QD ground state emission at high injection currents and domination of shorter wavelength peaks due to the excited states and the wetting layer [24]. In contrast, in QWDs, the ground state optical gain does not saturate up to very high injection currents [21], which can facilitate the realization of broadband emission and high output power. We expect that optimization of the active region by placing QWD layers with low carrier localization energy close to p-cladding would enable further increase in emission linewidth. Output power can be increased by using large cavity lengths, antireflection coatings, tapered lateral waveguides and multi-section designs, including those with an integrated optical amplifier.

Author Contributions: Conceptualization M.V.M., N.Y.G. and A.E.Z.; formal analysis, Y.M.S., G.O.K. and A.S.P.; funding acquisition, N.Y.G.; investigation, Y.M.S., G.O.K., A.A.B., S.A.M., N.A.K. and M.M.K.; methodology, A.S.P., A.A.B., S.A.M., N.A.K. and M.M.K.; project administration, M.V.M. and A.E.Z.; resources, A.S.P., A.A.B., S.A.M., N.A.K. and M.M.K.; supervision, M.V.M. and A.E.Z.; validation, Y.M.S., A.S.P., G.O.K., A.A.B., S.A.M., N.A.K. and M.M.K.; visualization, N.Y.G., G.O.K. and Y.M.S.; writing—original draft, M.V.M.; writing—review and editing, M.V.M., N.Y.G. and A.E.Z. All authors have read and agreed to the published version of the manuscript.

Funding: This work was supported by the Russian Science Foundation (project #23-72-00038).

Institutional Review Board Statement: Not applicable.

Informed Consent Statement: Not applicable.

Data Availability Statement: The data that support the findings of this study are available upon reasonable request from the authors.

Acknowledgments: Optical measurements have been performed, in part, in a large-scale research facility Complex Optoelectronic Stand operated by HSE University.

Conflicts of Interest: The authors declare no conflict of interest.

References

1. Hale, G.M.; Querry, M.R. Optical constants of water in the 200-nm to 200-μm wavelength region. *Appl. Opt.* **1973**, *12*, 555. [CrossRef]
2. Yasuno, Y.; Hong, Y.; Makita, S.; Yamanari, M.; Akiba, M.; Miura, M.; Yatagai, T. In vivo high-contrast imaging of deep posterior eye by 1-μm swept source optical coherence tomography and scattering optical coherence angiography. *Opt. Express* **2007**, *15*, 6121. [CrossRef] [PubMed]
3. Lv, X.Q.; Liu, N.; Jin, P.; Wang, Z.G. Broadband emitting superluminescent diodes with InAs quantum dots in AlGaAs matrix. *IEEE Photonics Technol. Lett.* **2008**, *20*, 1742. [CrossRef]
4. Yao, R.; Weir, N.; Lee, C.-S.; Guo, W. Broadband chirped InAs quantum-dot superluminescent light-Emitting diodes with $In_xAl_{1-x}As$ strain-reducing layers. *IEEE Photonics J.* **2016**, *8*, 1. [CrossRef]
5. Haffouz, S.; Barrios, P.J.; Normandin, R.; Poitras, D.; Lu, Z. Ultrawide-bandwidth, superluminescent light-emitting diodes using InAs quantum dots of tuned height. *Opt. Lett.* **2012**, *37*, 1103. [CrossRef]
6. Forrest, A.F.; Krakowski, M.; Bardella, P.; Cataluna, M.A. High-power quantum-dot superluminescent tapered diode under CW operation. *Opt. Express* **2019**, *27*, 10981. [CrossRef]
7. Zhang, Z.Y.; Hogg, R.A.; Xu, B.; Jin, P.; Wang, Z.G. Realization of extremely broadband quantum-dot superluminescent light-emitting diodes by rapid thermal-annealing process. *Opt. Lett.* **2008**, *33*, 1210. [CrossRef]
8. Han, I.K.; Bae, H.C.; Cho, W.J.; Lee, J.I.; Park, H.L.; Kim, T.G.; Lee, J.I. Study of chirped quantum dot superluminescent diodes. *Jpn. J. Appl. Phys.* **2005**, *44*, 5692. [CrossRef]
9. An, Q.; Jin, P.; Wu, J.; Wang, Z. Optical loss in bent-waveguide superluminescent diodes. *Semicond. Sci. Technol.* **2012**, *27*, 055003. [CrossRef]
10. Xin, Y.-C.; Martinez, A.; Saiz, T.; Moscho, A.J.; Li, Y.; Nilsen, T.A.; Gray, A.L.; Lester, L.F. 1.3-μm quantum-dot multisection superluminescent diodes with extremely broad bandwidth. *IEEE Photonics Technol. Lett.* **2007**, *19*, 501. [CrossRef]
11. Judson, P.D.L.; Groom, K.M.; Childs, D.T.D.; Hopkinson, M.; Hogg, R.A. Multi-section quantum dot superluminescent diodes for spectral shape engineering. *IET Optoelectron.* **2009**, *3*, 100. [CrossRef]
12. Ozaki, N.; Yamauchi, S.; Hayashi, Y.; Watanabe, E.; Ohsato, H.; Ikeda, N.; Sugimoto, Y.; Furuki, K.; Oikawa, Y.; Miyaji, K.; et al. Development of a broadband superluminescent diode based on self-assembled InAs quantum dots and demonstration of high-axial-resolution optical coherence tomography imaging. *J. Phys. D Appl. Phys.* **2019**, *52*, 225105. [CrossRef]
13. Wang, Z.C.; Jin, P.; Lv, X.Q.; Li, X.K.; Wang, Z.G. High-power quantum dot superluminescent diode with integrated optical amplifier section. *Electron. Lett.* **2011**, *47*, 1191. [CrossRef]
14. Rosetti, M.; Bardella, P.; Gioannini, M.; Montrosset, I. Carrier transport effects in multi layer quantum dot lasers and SLDs. In Proceedings of the ECIO'08 Eindhoven—14th European Conference on Integrated Optics and Technical Exhibition, Eindhoven, The Netherlands, 11–13 June 2008.
15. Guol, S.-H.; Wang, J.-H.; Wu, Y.-H.; Lin, W.; Yang, Y.-J.; Sun, C.-K.; Pan, C.-L.; Shi, J.-W. Bipolar cascade superluminescent diodes at the 1.04 μm wavelength regime. *IEEE Photonics Technol. Lett.* **2009**, *21*, 328–330. [CrossRef]
16. Heo, D.C.; Dong, S.J.; Choi, W.J.; Lee, J.I.; Jeong, J.C.; Han, I.K. Characteristics of superluminescent diodes utilizing $In_{0.5}Ga_{0.5}As$ quantum dots. *Jpn. J. Appl. Phys.* **2003**, *42*, 5133. [CrossRef]
17. Kovsh, A.; Krestnikov, I.; Livshits, D.; Mikhrin, S.; Weimert, J.; Zhukov, A. Quantum dot laser with 75 nm broad spectrum of emission. *Opt. Lett.* **2007**, *32*, 793. [CrossRef]
18. Lester, L.F.; Stintz, A.; Li, H.; Newell, T.C.; Pease, E.A.; Fuchs, B.A.; Malloy, K.J. Optical characteristics of 1.24—μm InAs quantum-dot laser diodes. *IEEE Photonics Technol. Lett.* **1999**, *11*, 931. [CrossRef]
19. Chen, S.; Li, W.; Zhang, Z.; Childs, D.; Zhou, K.; Orchard, J.; Kennedy, K.; Hugues, M.; Clarke, E.; Ross, I.; et al. GaAs-based superluminescent light-emitting diodes with 290-nm emission bandwidth by using hybrid quantum well/quantum dot structures. *Nanoscale Res. Lett.* **2015**, *10*, 340. [CrossRef]
20. Maximov, M.V.; Nadtochiy, A.M.; Mintairov, S.A.; Kalyuzhnyy, N.A.; Kryzhanovskaya, N.V.; Moiseev, E.I.; Gordeev, N.Y.; Shernyakov, Y.M.; Payusov, A.S.; Zubov, F.I. Light emitting devices based on quantum well-dots. *Appl. Sci.* **2020**, *10*, 1038. [CrossRef]
21. Gordeev, N.Y.; Maximov, M.V.; Payusov, A.S.; Serin, A.A.; Shernyakov, Y.M.; Mintairov, S.A.; Kalyuzhnyy, N.A.; Nadtochiy, A.M.; Zhukov, A.E. Material gain of InGaAs/GaAs quantum well-dots. *Semicond. Sci. Technol.* **2021**, *36*, 015008. [CrossRef]
22. Maximov, M.; Gordeev, N.; Shernyakov, Y.; Payusov, A.; Mintairov, S.; Kalyuzhnyy, N.; Kornyshov, G.; Serin, A.; Usikova, A.; Gadzhiev, I.; et al. Optoelectronic devices with active region based on InGaAs/GaAs quantum well dots. In Proceedings of the SPIE 11356, Semiconductor Lasers and Laser Dynamics IX, 113560A, Online, 20 April 2020. [CrossRef]
23. Kyaw, A.S.M.; Kim, D.-H.; Butler, I.M.; Nishi, K.; Takemasa, K.; Sugawara, M.; Childs, D.T.D.; Hogg, R.A. Extreme temperature operation for broad bandwidth quantum-dot based superluminescent diodes. *Appl. Phys. Lett.* **2023**, *122*, 031104. [CrossRef]
24. Markus, A.; Chen, J.X.; Paranthoe, C.; Fiore, A.; Platz, C.; Gauthier-Lafaye, O. Simultaneous two-state lasing in quantum-dot lasers. *Appl. Phys. Lett.* **2003**, *82*, 1818. [CrossRef]